Extratropical Impacts on Atlantic Tropical Cyclone Activity

GAN ZHANG AND ZHUO WANG

Department of Atmospheric Sciences, University of Illinois at Urbana–Champaign, Urbana, Illinois

TIMOTHY J. DUNKERTON

NorthWest Research Associates, Inc., Bellevue, Washington

MELINDA S. PENG

Naval Research Laboratory, Monterey, California

GUDRUN MAGNUSDOTTIR

Department of Earth System Science, University of California, Irvine, Irvine, California

(Manuscript received 12 June 2015, in final form 11 December 2015)

ABSTRACT

With warm sea surface temperature (SST) anomalies in the tropical Atlantic and cold SST anomalies in the east Pacific, the unusually quiet hurricane season in 2013 was a surprise to the hurricane community. The authors' analyses suggest that the substantially suppressed Atlantic tropical cyclone (TC) activity in August 2013 can be attributed to frequent breaking of midlatitude Rossby waves, which led to the equatorward intrusion of cold and dry extratropical air. The resultant mid- to upper-tropospheric dryness and strong vertical wind shear hindered TC development. Using the empirical orthogonal function analysis, the active Rossby wave breaking in August 2013 was found to be associated with a recurrent mode of the midlatitude jet stream over the North Atlantic, which represents the variability of the intensity and zonal extent of the jet. This mode is significantly correlated with Atlantic hurricane frequency. The correlation coefficient is comparable to the correlation of Atlantic hurricane frequency with the main development region (MDR) relative SST and higher than that with the Niño-3.4 index. This study highlights the extratropical impacts on Atlantic TC activity, which may have important implications for the seasonal predictability of Atlantic TCs.

1. Introduction

Atlantic tropical cyclone (TC) activity exhibits substantial interannual variability. The interannual variability is closely related to tropical climate modes, such as the El Niño–Southern Oscillation (ENSO; e.g., Gray 1984a) and the Atlantic Meridional Mode (AMM; e.g., Kossin and Vimont 2007), which are characterized by the variability of tropical sea surface temperature (SST). Recent studies also found that the Atlantic TC frequency and the accumulated cyclone energy (ACE; Bell et al. 2000) are closely related to the SST anomalies in the Atlantic main development region (MDR; Goldenberg et al. 2001) relative to the global tropical mean (e.g., Latif et al. 2007; Vecchi and Soden 2007; Swanson 2008) or relative to the tropical Indo-Pacific (Lee et al. 2011). Given the strong correlations, the slowly varying SST in the tropics serves as an important predictor in the seasonal prediction of Atlantic TCs (e.g., Gray 1984b; Vecchi et al. 2014).

The seasonal forecast of Atlantic TC frequency has been proved skillful in recent years. The statistical prediction dates back to the 1980s. The model developed by Dr. William Gray and colleagues (Gray 1984b; Klotzbach and Gray 2009), which evolved over the years, employs predictors including an ENSO index and the SST in the tropical or subtropical Atlantic. Besides the statistical method, the dynamical approach, and the statistical–dynamical hybrid approach have attracted increasing attention and shown competitive skill (Vitart

Corresponding author address: Zhuo Wang, Dept. of Atmospheric Sciences, University of Illinois at Urbana–Champaign, 105 S. Gregory St., Urbana, IL 61801.
E-mail: zhuowang@illinois.edu

DOI: 10.1175/JAS-D-15-0154.1

et al. 2007; H. Wang et al. 2009; LaRow et al. 2010; Kim and Webster 2010; Chen and Lin 2011, 2013; Vecchi et al. 2014). Among these studies, Zhao et al. (2010) and Chen and Lin (2011, 2013) carried out hindcasts with an atmospheric general circulation model (AGCM) driven by the persistent SST anomalies, and the hindcasts captured the interannual variations of Atlantic TC activity with remarkable skill. The hybrid model devised by Vecchi et al. (2014) employed the relative SST in the MDR as the sole predictor in a Poisson regression model, and the forecast skill is comparable to or even better than some dynamical forecasts. The success of these forecast schemes highlights the strong (direct and indirect) control of tropical SST on Atlantic TC activity.

The tropical SST control of TC activity can be explained by the empirical relationship between tropical SST and large-scale atmospheric conditions. The established knowledge suggests that Atlantic TCs are impacted by vertical wind shear (VWS), midlevel moisture, and tropical easterly waves (e.g., DeMaria 1996; Goldenberg and Shapiro 1996). Their contributions can be integrated in the framework of the regional Hadley circulation (Zhang and Wang 2013; Wang et al. 2015). Zhang and Wang (2013) found that the leading interannual mode of the Atlantic Hadley circulation, which is associated with variations of the ITCZ intensity and width, is strongly correlated with Atlantic hurricane activity ($r \approx 0.7$ for 1979–2010) and that this mode is modulated by SST anomalies in the tropical and subtropical Atlantic as well as the tropical Pacific.

Despite the improvements of seasonal prediction in recent years, it is worth pointing out that a substantial amount of TC variability is not captured by forecast schemes. For example, a correlation coefficient of 0.7 between the observed storms and the forecasts indicates that the forecasts only capture about 50% of the total variance. Furthermore, dynamical models show that AGCM ensembles, even when driven by the same SST forcing, exhibit a large spread in the predicted hurricane counts (e.g., Chen and Lin 2013). This suggests that the internal variability of the atmosphere or forcing other than the tropical SST, which are not included in statistical schemes or not well captured by dynamical models, may have significant impacts on the TC activity.

A notable seasonal forecast bust of Atlantic TC activity occurred in 2013. The hurricane season was preceded by warm SST anomalies in the tropical Atlantic and cold SST anomalies in the equatorial east Pacific, which persisted through the hurricane season (see Fig. 2a and discussion in section 3). Both were expected to contribute to an active hurricane season. Furthermore, African easterly waves (AEWs) in August and September were very active over West Africa and the east Atlantic, which typically contributes to an active hurricane season (Hopsch et al. 2007). Despite these favorable conditions, a hurricane-strength tropical storm failed to develop until 11 September; only two short-lived hurricanes developed in the season and neither of them became major hurricanes; Blunden and Arndt 2014). The lack of hurricanes in August and early September was particularly remarkable because this period typically contributes 50% to the seasonal ACE. As a result of the absence of hurricanes in August and early September, the ACE was only ~20% of the climatological value in early September 2013 (Fig. 1). The extremely low hurricane number and low ACE in 2013 were in sharp contrast with the seasonal predictions from various institutions (see the appendix), and the quietness of the season was a topic of hot debate on the tropical storms mailing list (http://tstorms.org/).

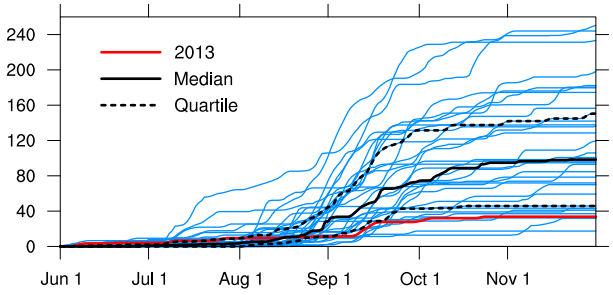

FIG. 1. ACE as a function of calendar dates. The daily ACE values (10^4 knots^2; 1 kt = 0.51 m s^{-1}) are calculated for the entire Atlantic basin using the best track dataset. The red curve represents 2013, and blue curves represent other years during 1979–2012. The figure format is adapted from Brian McNoldy (*Washington Post*, 25 Nov 2013).

As shown later in section 3, the suppressed TC activity can be attributed to the hostile atmospheric conditions, and the forecast bust in 2013 thus indicates the breakdown of the empirical relations between tropical SST and the atmospheric conditions modulating TC activity, which are key to the success of many seasonal prediction models. It is interesting to ask what contributed to the unfavorable atmospheric conditions and disrupted the empirical relations between tropical SST and Atlantic TCs in 2013 and what may be missing in forecast schemes. Investigation of these questions, which motivates this study, will lead to a better understanding of the variability and predictability of Atlantic TCs and has the potential to improve seasonal predictions.

In the next section, we will briefly describe the data and methods used in this study. Section 3 provides an overview of large-scale environmental conditions in the 2013 Atlantic hurricane season. A case study is presented in section 4. The impacts of Rossby wave

breaking (RWB) on Atlantic TCs and the association with the midlatitude mean flow are examined in section 5. The last section provides a summary.

2. Data and methods

a. Data

The ERA-Interim "dataset" (http://apps.ecmwf.int/datasets/) from the period 1979–2013 (Dee et al. 2011) is employed to examine the atmospheric conditions. The 6-hourly and monthly mean data on isobaric and isentropic levels are used, and the horizontal grid spacing of the data is about 0.7° (unless otherwise specified). To examine the tropical easterly wave activity, we derived eddy kinetic energy (EKE) from the 2.5–9-day bandpass (Doblas-Reyes and Déqué 1998) filtered wind data. Additionally, we used SST data from the HadISST (Rayner et al. 2003), the NOAA Atlantic hurricane best track dataset (Landsea and Franklin 2013), and the climate indices archived by NOAA/PSD (http://www.esrl.noaa.gov/psd/data/climateindices/list/). Although the strong suppression of Atlantic hurricane activity (Fig. 1) persisted from August to early September in 2013, we focus on August in the following analysis to facilitate data processing and comparison with previous studies.

b. Detection of Rossby wave breaking

RWB occurs when Rossby waves propagate into a region where the background flow cannot provide adequate support for the linear wave propagation. This results in increased wave amplitude followed by the rapid and irreversible overturning of potential vorticity (PV) contours or RWB (McIntyre and Palmer 1983). RWB can be categorized as the cyclonic type or anticyclonic type based on the direction of breaking (Thorncroft et al. 1993). In the hurricane season, the anticyclonic RWB dominates the equatorward flank of the midlatitude jet over the North Atlantic (Postel and Hitchman 1999; Abatzoglou and Magnusdottir 2006) and is the focus of this study.

To identify the anticylonic RWB objectively and evaluate its frequency, we employ the RWB detection algorithm described in Abatzoglou and Magnusdottir (2006) and Strong and Magnusdottir (2008). First the ERA-Interim PV data are coarsened to a 2.5° × 2.5° resolution grid. We focus on the 350-K isentropic surface and identify the longest circumpolar PV contour for PV values between 1.5 and 7.0 PV units (PVU) at 0.5-PVU intervals (1 PVU = $10^{-6}\,m^2\,s^{-1}\,K\,kg^{-1}$; 12 PV contours in total). We then search the circumpolar contours for the PV contour that crosses a meridian more than once, which is denoted as the PV overturning. The detected overturning is counted as one RWB incidence, and the location and zonal extent of the breaking bay (the equatorward tongue of high-PV air) is extracted. To investigate the spatial distribution of RWB, we locate the RWB centroids and count the frequency of RWB occurrence on a 5° × 5° resolution grid mesh.

3. Overview of the environmental conditions in August 2013

a. Monthly means

The SST anomalies in August 2013 are shown in Fig. 2a. Positive SST anomalies prevail over the tropical and subtropical Atlantic, and cold anomalies are present in the east Pacific, resembling a La Niña pattern (Fig. 2a). The MDR warming and the east Pacific cooling, suggesting a relative SST warming in the MDR, favor TC development by destabilizing the atmosphere and reducing VWS (e.g., Vecchi and Soden 2007). Given the SST pattern, one would expect elevated TC activity in August 2013, which is opposite to the observation (Fig. 1).

The VWS anomalies are shown in Fig. 2b. VWS is defined here as the magnitude of the vector difference between 200- and 850-hPa monthly mean wind fields [$\mathrm{VWS} = \sqrt{(u_{200} - u_{850})^2 + (v_{200} - v_{850})^2}$]. A positive (negative) anomaly means that the shear is stronger (weaker) than the climatological mean. Figure 2b shows that VWS is stronger than the climatological mean in most regions of the tropical and subtropical Atlantic, especially over the Greater Antilles ($>5\,m\,s^{-1}$). Strong VWS over the tropical Atlantic is typically associated with warm SST anomalies in the equatorial east Pacific (e.g., Gray 1984a; Goldenberg and Shapiro 1996; Aiyyer and Thorncroft 2006). However, the observed cooling in the equatorial east Pacific suggests that this empirical relation breaks in August 2013.

Another factor that affects TC formation is the tropospheric moisture distribution. With the ERA-Interim data, we derived the free-tropospheric precipitable water (PW; 200–850 hPa) and examined the August 2013 anomalies. Figure 2c shows a band of dry anomalies extending southwestward from the Azores to the Central MDR and the subtropical west Atlantic. Negative anomalies also appear over the Guinea coast, while positive anomalies prevail over the subtropical east Atlantic and West Africa. The moisture anomalies are largely consistent with tropical rainfall anomalies (not shown). In particular, the West African monsoon extends more northward than average and generates more rainfall over the Sahel. Although previous studies showed that Sahel rainfall is positively correlated with

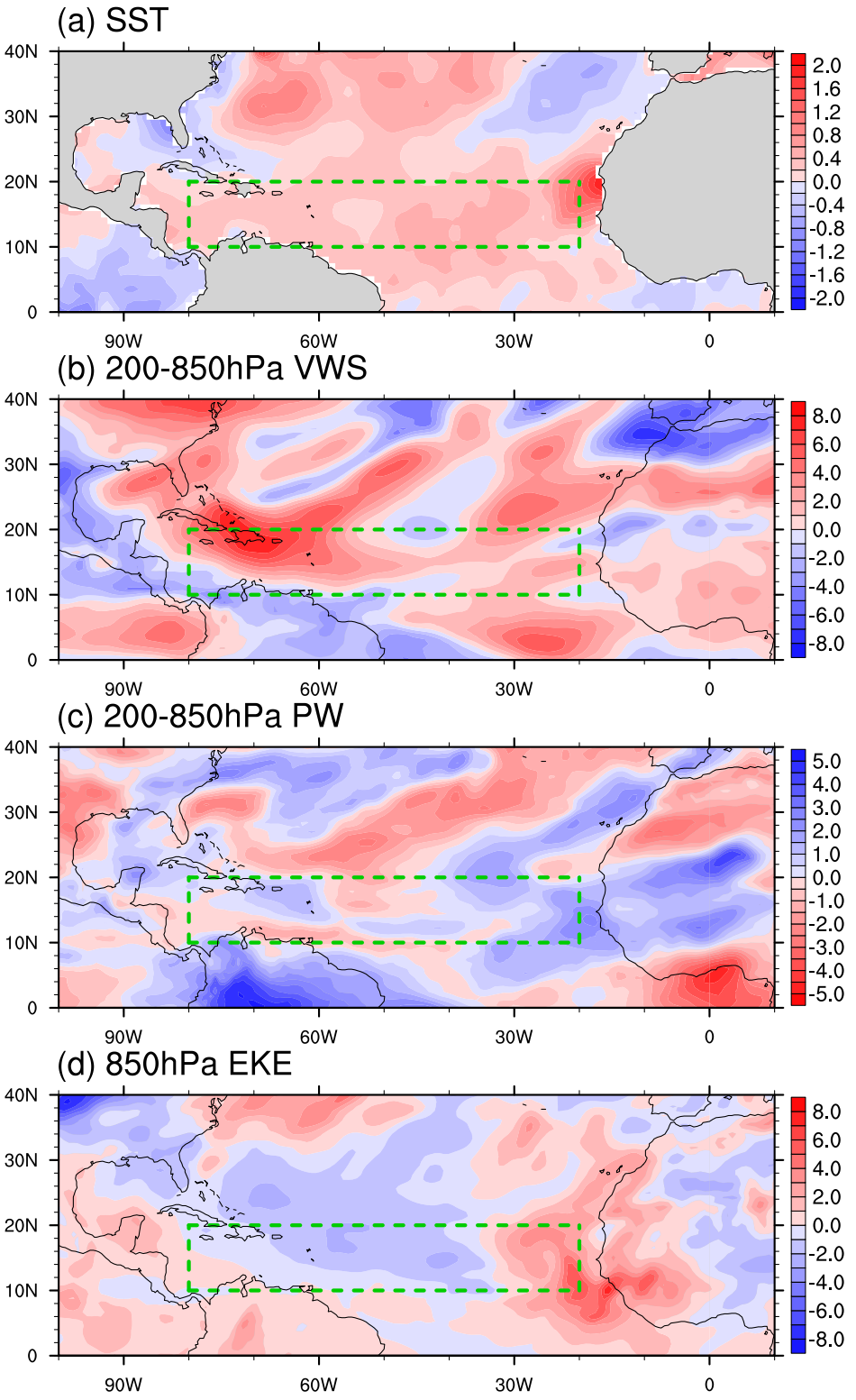

FIG. 2. Monthly mean anomalies in August 2013. (a) Sea surface temperature (K); (b) magnitude of vertical wind shear (200–850 hPa; $m\,s^{-1}$); (c) precipitable water (200–850 hPa; mm); and (d) 850-hPa eddy kinetic energy (2.5–9-day bandpass; $m^2\,s^{-2}$). The climatology is the long-term mean during 1981–2010. The green box highlights the Atlantic MDR (10°–20°N, 20°–80°W).

Atlantic TC activity (e.g., Gray 1990), such a relationship did not hold in August 2013.

The EKE anomalies (Fig. 2d) suggest that AEWs are anomalously active over West Africa and the east Atlantic but relatively inactive west of 40°W. This is consistent with the authors' impression in the real-time wave tracking that tropical easterly waves tended to weaken over the central Atlantic (http://www.met.nps.edu/~mtmontgo/storms2013.html). The distribution of PV at the 315-K isentropic surface suggests that easterly waves tend to be directed poleward east of 40°W (not shown; see Tyner and Aiyyer 2012 for more discussion). The poleward recurvature of the wave track into the subtropics, with low humidity, strong VWS, and cold SST, may contribute to reduced hurricane activity in 2013 (Elsner 2003; Kossin et al. 2010).

Overall, the analyses suggest that tropical Atlantic atmospheric conditions in August 2013 cannot be explained by the tropical SST anomalies. Meanwhile, the time series of the all-season real-time multivariate MJO index suggest that the impacts of the MJO were very weak except in late August (http://www.bom.gov.au/climate/mjo/). Since our real-time wave tracking suggests that the west and central Atlantic is a crucial region for the suppression of hurricane activity, we will focus on this region and further examine the VWS and tropospheric humidity anomalies in the next subsection.

b. *Probability distribution analyses*

Figures 2b and 2c show that dryness and high VWS extend southwestward from extratropics to the west and central Atlantic. On the other hand, the probability distribution of humidity often shows a bimodal structure (Yang and Pierrehumbert 1994; Brown and Zhang 1997; Zhang et al. 2003), and the anomalies may not be well represented by a monthly mean field. To better illustrate the extreme conditions in humidity and VWS on the synoptic time scale, we derived a joint probability distribution function (PDF) of PW and VWS in the west MDR (10°–20°N, 40°–80°W) using the 6-hourly ERA-Interim data (Fig. 3).

The bimodal distribution of moisture is discernible in the PDF of PW in August 2013 (the red curve in Fig. 3a). Compared to the climatological mean PDF, dry air (PW $\leq$ 15 mm) occurred more frequently in 2013, and the frequency of moist conditions (PW $>$ 20 mm) is reduced. The pronounced changes, however, are not well represented by the areal mean (vertical black lines in Figs. 3a,b). Meanwhile, the joint PDF anomalies (Fig. 3c) show the frequent concurrence of dryness and high-shear conditions (upper-left part of plotting space). The combination of strong VWS and dry air can effectively hinder TC formation and intensification (e.g., Tang and Emanuel 2012; Fritz and Wang 2013; Ge et al. 2013).

To illustrate better the vertical distribution of moisture anomalies in the west MDR, we use the contoured frequency with altitude diagram (CFAD) to analyze the relative humidity (Figs. 3d–f). The tripole-like pattern of anomalies in the middle troposphere (500–850 hPa) indicates the frequent occurrence of both extremely dry and moist conditions. In the upper troposphere (200–500 hPa), the most striking feature is the increasing occurrence of extreme dryness (RH $<$ 10%). Similar to the midtropospheric dryness, the upper-tropospheric dry air can also suppress deep convection (Takemi et al. 2004; Jensen and Del Genio 2006; Wang et al. 2012). The mid- to upper-tropospheric dry air, when present ahead of the wave trough, hinders the TC development in an easterly wave (Hopsch et al. 2010; Hankes et al. 2014). This is probably due to the absence of a quasi-closed Lagrangian circulation at the early stage of TC development (Fritz and Wang 2013).

The vertical distribution of moisture anomalies hints at the origin of the dry air. Dry air over the tropical Atlantic is typically associated with the Saharan air layer (SAL) or midlatitude air intrusions (Dunion 2011). The SAL, which is characterized by high dust/aerosol concentration, contributes to the dryness below 500 hPa but tends to increase the relative humidity in the mid- and upper troposphere (Braun 2010), which is different from Figs. 3d–f. In contrast, midlatitude intrusions often contribute to extremely dry air (RH $<$ 10%) in the upper troposphere (Waugh 2005), with strong impacts on summertime convection in North Africa and the tropical North Atlantic (e.g., Roca et al. 2012). In addition, extratropical dry air intrusions are also accompanied by strong VWS during the Atlantic hurricane season (Dunion 2011). The characteristics of humidity and VWS features thus imply the anomalies in August 2013 may be related to the extratropical processes.

4. A case study

To understand better the processes contributing to the concurrence of dry and strong-VWS conditions, we examine a dry air outbreak event in August 2013. PV on the 350-K isentropic surface, along with other variables, is examined to study the dynamical and thermodynamical processes.

Figures 4a–c show the snapshots of PV at 1200 UTC 11 August, 0000 UTC 14 August, and 1200 UTC 16 August, respectively. Before 1200 UTC 11 August, a

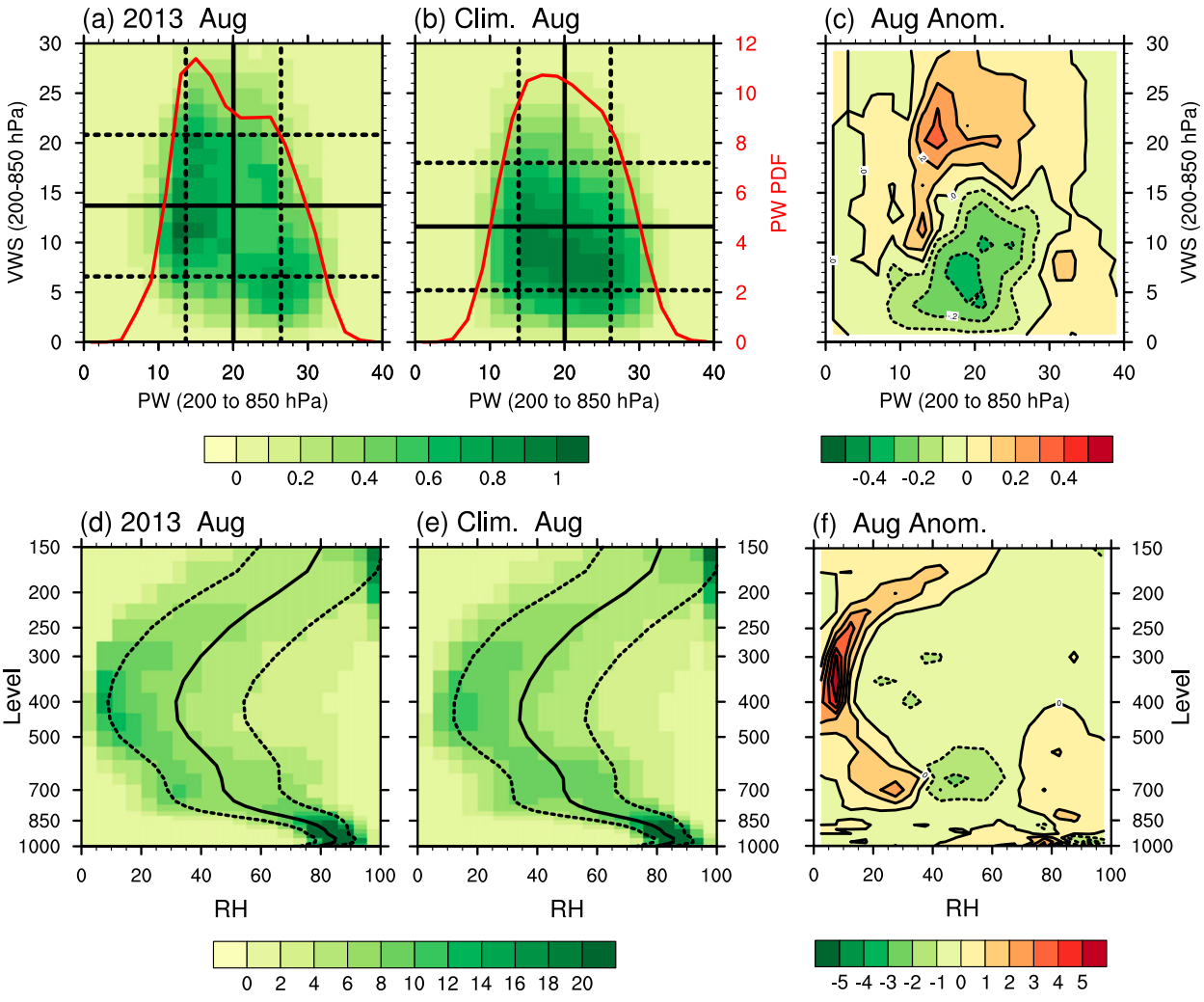

FIG. 3. PW (200–850 hPa; mm) and VWS (200–850 hPa; m s^{-1}) distribution in the western MDR (10°–20°N, 40°–80°W) during August 2013. (a)–(c) Two-dimensional PDF (%) of PW and VWS. (d)–(f) CFAD (%) of relative humidity (%). (left)–(right) Plots for August 2013, August climatology (1981–2010), and their differences. In (left) and (middle), solid and dashed black lines represent mean and one standard deviation range, respectively. In (right), thin solid and dashed black contours represent positive and negative values, while the thick solid contour is the zero contour. The intervals are 0.1% in (c) and 1% in (f). The red lines and axis in (a) and (b) represent the one-dimensional PDF (%) of PW, and the coordinate (red) is marked on the right of (b).

Rossby wave propagates eastward along the strong PV gradient associated with the tropopause at 350 K. It gradually amplifies and extends equatorward. Wave breaking occurs as the wave encounters the weaker westerly flow equatorward of the midlatitude jet. The breaking results in two high-PV centers at 1200 UTC 11 August, denoted as P1 (45°N, 35°W) and P2 (33°N, 53°W), respectively (Fig. 4a). P1 and P2 stagger in the weak westerly flow and slowly move equatorward. At 0000 UTC 14 August (Fig. 4b), P1 is located near 30°N, 60°W and has weakened significantly. Meanwhile, P2 continues staggering around 35°N, 25°W and persists well beyond 1200 UTC 16 August before remerging with the extratropical high-PV reservoir.

RWB contributes to mixing between the dry extratropical air and moist tropical air (Figs. 4d–f). High moisture content is found in the ITCZ and monsoon regions, while dry air prevails in the extratropics, except where a moisture plume extends northeastward from the North America monsoon region. The collocated dry air and PV filaments indicate the mixing of dry extratropical air of high PV with moist tropical air of low PV. Over the east Atlantic, the equatorward transport of extratropical dry air may be further aided by the subtropical anticyclonic circulation (Cau et al. 2007). As shown in Figs. 4d–f, an outbreak of extremely dry air near the African coast, contributed by RWB, extends southwestward into the MDR by 0000 UTC 14 August. The dry air

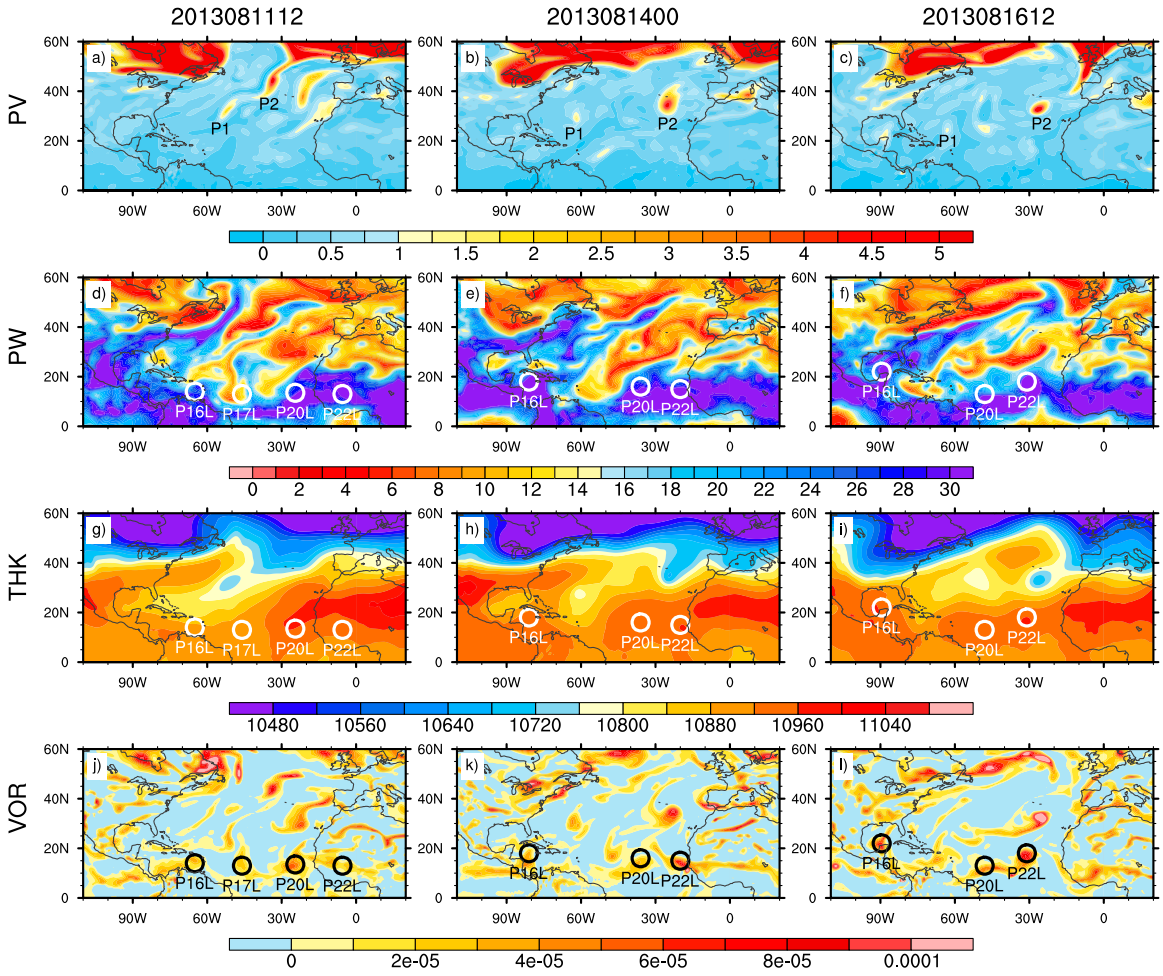

FIG. 4. Evolution of a midlatitude RWB event: (a)–(c) 350-K PV (PVU), (d)–(f) 200–850-hPa PW (mm), (g)–(i) 200–850-hPa thickness (THK; m), and (j)–(l) 700-hPa relative vorticity (VOR; s^{-1}). The times are (left)–(right) 1200 UTC 11 Aug, 0000 UTC 14 Aug, and 1200 UTC 16 Aug 2013, at 60-h intervals. P1 and P2 in the PV plots denote the two high-PV centers resulting from RWB; the circles in PW, THK, and VOR plots denote easterly wave pouches (the naming convention for the pouches follow http://www.met.nps.edu/~mtmontgo/storms2013.html).

later sweeps westward and reduces the tropospheric moisture over the Caribbean by 1200 UTC 16 August.

RWB also contributes to cold temperature anomalies over the tropical and subtropical Atlantic, as suggested by the 200–850-hPa thickness (Figs. 4g–i). The high-PV air resulting from RWB often collocates with low thickness. As shown in Figs. 4g–i, the cold air (of low thickness) associated with P1 and P2 extends southwestward from the midlatitudes to the Greater Antilles along the Atlantic tropical upper-tropospheric trough (TUTT; Fitzpatrick et al. 1995). The south edge of this cold tongue has a sharp temperature gradient, implying strong VWS under the thermal wind relation (Holton 2004).

The dry air and strong VWS associated with RWB may hinder tropical cyclogenesis from easterly waves, as demonstrated in the evolution of four wave pouches (marked with circles in Fig. 4). A wave pouch is a region of quasi-closed Lagrangian circulation in the lower free troposphere within a synoptic-scale wave, straddling the intersection of wave trough and the critical latitude. Previous studies suggested that the pouch center is the preferred location for tropical cyclogenesis in tropical easterly waves (e.g., Dunkerton et al. 2009; Z. Wang et al. 2009). At 1200 UTC 11 August, four wave pouches, P16L, P17L, P20L and P22L, are present over the Atlantic MDR and West Africa. While P16L, P20L and P22L are located in a moist environment, P17L is located in a region of dry air associated with a previous RWB event. The strong thickness gradient along the southern boundary of the cold tongue (Fig. 4g) indicates that both P16L and P17L are in close proximity to strong VWS. P17L diminishes quickly, while the other pouches continue to travel westward (Fig. 4h). Although P16L later

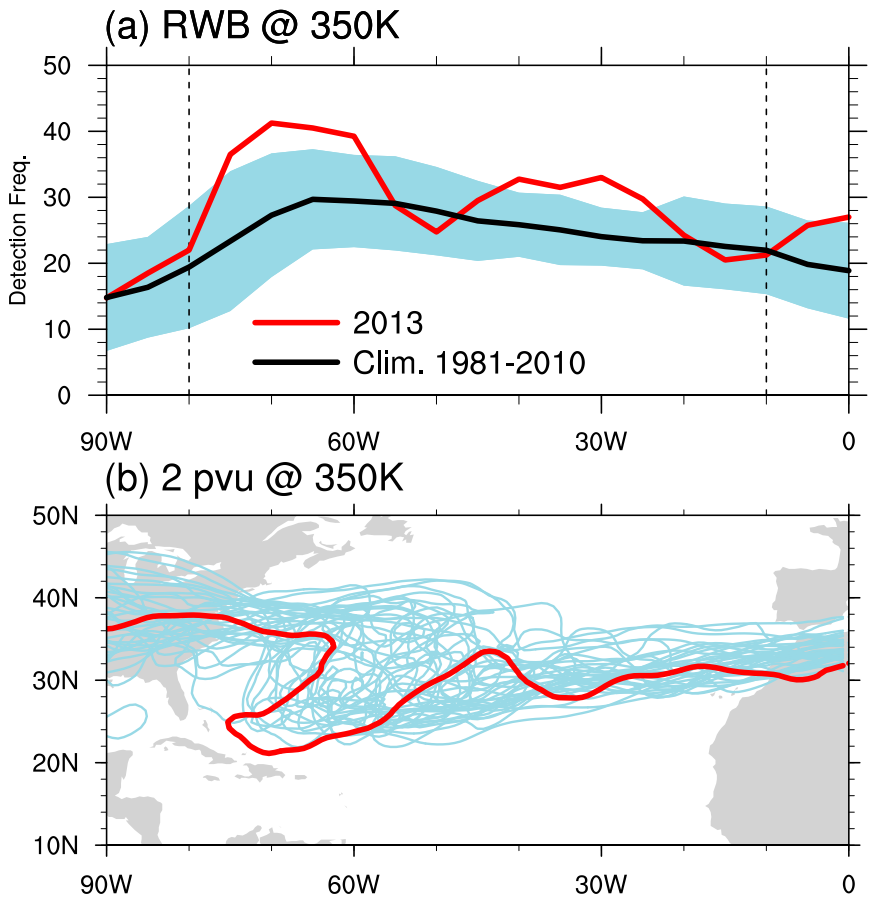

FIG. 5. (a) Anticyclonic RWB frequency between 20° and 40°N as a function of longitude for August 2013 (red curve) and the long-term mean (black); blue shading represents one standard deviation from the mean (1981–2010). Vertical dashed lines highlight 10° and 80°W. (b) The 2-PVU contours on the 350-K surface. Red represents 2013 and blue represents the other years in 1979–2013.

escapes from the impacts of strong VWS and dry air, it does not have enough time to intensify before moving over to land.

P20L is accompanied by dry air to its west at 1200 UTC 11 August, and the convection associated with the wave is weak or scattered most of the time as P20L propagates over the east and central Atlantic (see http://www.met.nps.edu/~mtmontgo/archive2013.html). Although convection is reinvigorated when P20L moves to the west Caribbean and the system manages to develop into Tropical Storm Fernand over the Gulf, it does not have time to further intensify before making landfall on 26 August.

P22L is embedded in a deep layer of moisture at 1200 UTC 11 August and 0000 UTC 14 August (Figs. 4d,e). It develops into Tropical Storm Erin near the Cape Verde Islands, the only TC over the east Atlantic in August 2013. Erin then recurves northwestward and encounters the residual flow of the P2. As a result of the dry air and strong VWS (not shown; see Cangialosi 2013), Erin soon weakens into a tropical low on 18 August, lasting only about three days.

5. Rossby wave breaking and Atlantic tropical cyclones

a. Impacts of Rossby wave breaking

The case study in section 4 suggests that the anticyclonic RWB may hinder the TC formation and intensification by reducing tropospheric moisture and enhancing VWS. Similar RWB events happened repeatedly over the west and east Atlantic from August to mid-September in 2013. It is then natural to ask whether RWB was particularly active in August 2013.

Using the detection algorithm described in section 2b, we evaluated the anticyclonic RWB frequency between 20°–40°N, equatorward of the midlatitude jet axis. The RWB frequency in August 2013 was plotted as a function of longitude in Fig. 5a. Also plotted is

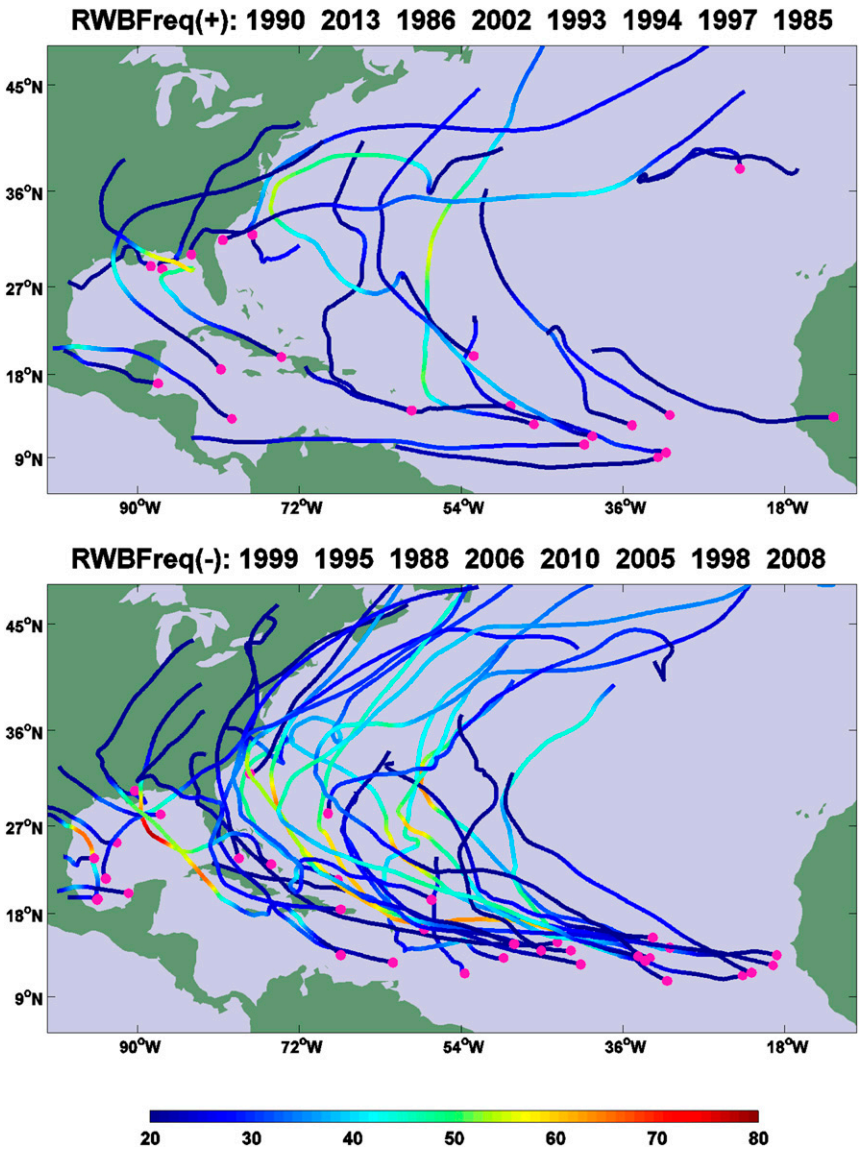

FIG. 6. Tropical cyclone track composites for the (top) positive and (bottom) negative phases of RWBFreq. The composite years are listed on the top of each panel, following the descending order of RWBFreq anomaly magnitude. Pink dots denote the genesis locations, and colors along tracks denote represent the storm intensity in terms of the maximum surface wind speed ($m\,s^{-1}$).

the long-term mean and standard deviation. This figure confirmed that RWB was indeed more active in August 2013 over the North Atlantic. Active RWB was found over both the western basin (~65°W) and the eastern basin (~30°W). Along with the active RWB, the 2-PVU contour is displaced equatorward over the west Atlantic. The displacement is related to an amplified high-PV tongue or a stronger TUTT over the west Atlantic, which can be attributed to the frequent RWB in this area (Postel and Hitchman 1999).

To confirm the impacts of RWB on Atlantic tropical cyclones, we defined an index, RWBFreq, based on the anticyclonic RWB frequency equatorward of the midlatitude jet core: the RWB frequency was summed over 10°–90°W, between 10° south of the jet axis (August climatology in 1981–2010) and 10°N. The area is outlined in Fig. 8b (below) by green lines, and small variations of the boundaries do not qualitatively affect the findings presented below. Composites of TC tracks were constructed based on the index (Fig. 6). In the eight years of strongest positive RWBFreq anomalies, the TC

TABLE 1. Correlation coefficients of the Atlantic hurricane frequency (HurrN), tropical storm frequency (TSN), and ACE with different indices in August 1979–2013: RWBFreq, MDR SST (MDR; 10°–20°N, 20°–80°W), MDR relative SST (RSST; Vecchi and Soden 2007), Niño-3.4, Sahel rainfall (SahelR; Janowiak 1988), first mode of the Atlantic Hadley circulation (HC1; Zhang and Wang 2013), the NAO/CPC index (Barnston and Livezey 1987), and the NAO/Jones index (Jones et al. 1997). Correlations exceeding the 95% confidence level are in boldface.

	HurrN	TSN	ACE
RWBFreq	**−0.47**	**−0.39**	**−0.49**
MDR	**0.43**	**0.54**	**0.47**
RSST	**0.50**	**0.57**	**0.50**
Niño-3.4	**−0.35**	−0.26	**−0.34**
SahelR	**0.34**	0.30	0.30
HC1	**−0.45**	**−0.36**	**−0.41**
NAO/CPC	−0.19	−0.23	−0.02
NAO/Jones	−0.21	−0.19	−0.26

track density is substantially reduced, especially over the MDR; the storms are generally weaker and shorter-lived: 21 TCs formed, 8 of which (38%) reached the hurricane intensity. In contrast, 35 TCs developed in the eight years of strongest negative RWBFreq anomalies, 18 of which (54%) strengthened into hurricanes.[1] There are also a larger number of TCs making landfall or impacting the U.S. East Coast in the negative phase of RWBFreq.

The linkage between RWB and Atlantic TC activity is consistent with correlation analyses (Table 1). RWBFreq is negatively correlated with indices of Atlantic TC activity, including hurricane frequency (−0.47), tropical storm frequency (−0.39), and ACE (−0.49). These correlations are remarkable when compared with other correlations in Table 1 and are statistically significant. Our analyses suggest that the frequent occurrence of anticyclonic RWB suppresses Atlantic TC activity, although PV filaments associated with RWB may occasionally lead to tropical cyclogenesis (Galarneau et al. 2015).

The linkage between RWB and Atlantic TC activity can be explained by the impacts of RWB on the atmospheric conditions affecting TC formation and intensification. We constructed the PDFs of the 850–200-hPa precipitable water and VWS over the western MDR for the positive and negative phases of the RWBFreq (Fig. 7; the same composite years as in Fig. 6). Compared to the negative phase, dry and high-VWS conditions occur more frequently in the positive phase, and moist and low-VWS conditions occur less frequently (Figs. 7a–c). In addition, the CFAD of relative humidity shows that dryness occurs more frequently between 300 and 850 hPa when RWB is more active over the west MDR (Figs. 7d–f). These anomalies resemble those in August 2013 and are consistent with suppressed TC activity in the positive phase of RWBFreq (Fig. 6).

b. *RWB and the mean flow*

The location and frequency of RWB have close association with the structure and intensity of the upper-level jets (e.g., Hartmann and Zuercher 1998; Scott et al. 2004), and the association is evident in August 2013. Figure 8 shows the monthly mean 200-hPa zonal wind in August 2013, the climatological mean, and their difference. Compared to the climatological mean, the midlatitude jet in August 2013 was stronger and has a larger strain rate on its equatorward flank. Such a sharpened jet is consistent with the PV staircase concept related to the strong PV stripping due to active RWB (Dritschel and McIntyre 2008; Dunkerton and Scott 2008). Another notable anomaly in Fig. 8c is the eastward extension of the midlatitude jet over the east Atlantic. Since the jet exit is one of the preferred regions for RWB (Nakamura 1994), the eastward extension is consistent with the active RWB over the east Atlantic in August 2013 (Fig. 5a).

It is natural to ask whether the findings for 2013 can be generalized and whether the extratropical anomalies in 2013 are associated with a recurrent extratropical mode that modulates Atlantic TC activity. Investigation of this issue helps to provide a large-scale perspective for the variability of the RWB occurrence and also helps to assess the potential predictability of RWB. Using the empirical orthogonal function (EOF) analysis, we extracted two leading modes in the interannual variability of the 200-hPa zonal wind (August 1979–2013; data detrended prior to the EOF analysis) over the North Atlantic (10°–80°N; 90°W–20°E). These two EOF modes (denoted as EOF1U and EOF2U, respectively) are characterized by activity centers over the extratropical Atlantic (Fig. 9) and explain 26.0% and 12.5% of the total variance, respectively.[2] The comparison between the EOF loading (color) and the climatology (contour) (Figs. 9a,b) suggests that EOF1U mainly represents a meridional displacement of the westerly jet

[1] Although the hurricane season was notably active in 2005, the number of tropical cyclones (five) or hurricanes (two) in August 2005 was comparable to the other years in the negative composite. Excluding 2005 thus does not affect our conclusions qualitatively.

[2] Similar modes were identified in other reanalysis datasets [e.g., NCEP–NCAR reanalysis during 1948–2013 (Kalnay et al. 1996)] and on different temporal resolution (e.g., 6-hourly data), indicating the robustness of EOF1U and EOF2U.

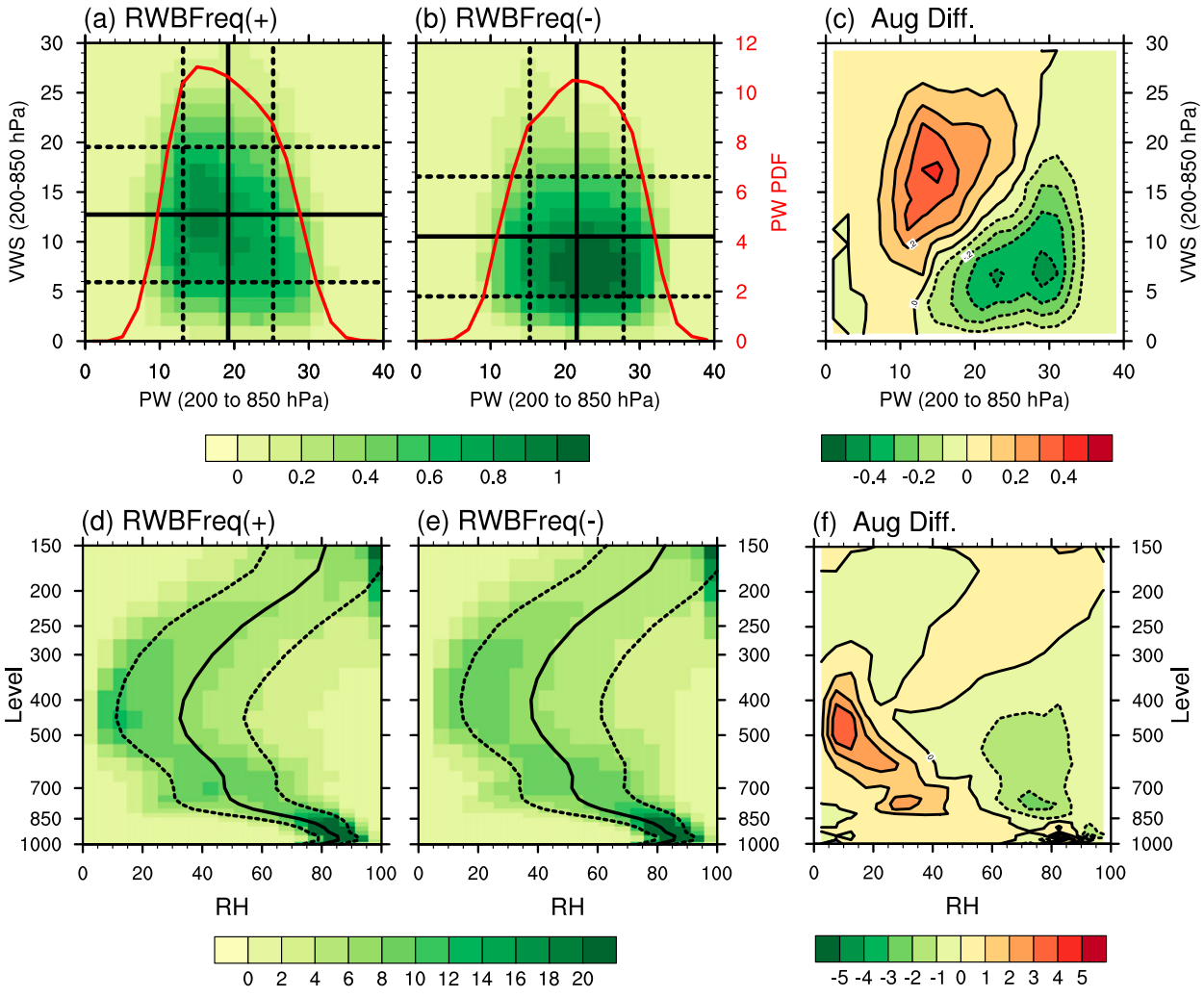

FIG. 7. As in Fig. 3, but the composites for the (a),(d) positive and (b),(e) negative phases of RWBFreq and (c),(f) their differences.

near the jet exit (Fig. 9a). Although EOF1U explains a substantial portion of extratropical variability, it does not have a significant correlation with Atlantic TC activity (Table 2). On the other hand, EOF2U modulates the intensity and zonal extent of the midlatitude jet, as well as the strain rate equatorward of the jet core (Fig. 9b). This mode loading resembles the anomalous pattern in August 2013 (Fig. 8c), and the time series of EOF2U shows that 2013 is a strong positive year (Fig. 9d). We will thus focus on EOF2U in the following analyses.

As expected, EOF2U is significantly correlated with RWBFreq. The association between EOF2U and the RWB occurrence is further illustrated by the composites of anticyclonic RWB distribution (Fig. 10). Figures 10a and 10b show that anticyclonic RWB mostly happens on the equatorward flank of the midlatitude jet and the jet exit region. In the positive phase of EOF2U, RWB tends to occur more frequently near the TUTT (25°N, 60°W) and the midlatitude jet exit (35°N, 25°W) (Fig. 10c). The significant differences, however, appear a little scattered, implying that the jet variations associated with EOF2U do not strongly constrain the longitudinal distribution of RWB. For example, in August 2005, a case with strong positive EOF2U, RWB occurred frequently over the east Atlantic but infrequently over the west Atlantic (figure not shown); RWB occurrence in August 2013, however, was frequent over both the east and west Atlantic (Fig. 5a).

Consistent with its association with RWB occurrence, EOF2U is significantly correlated with the hurricane frequency, and the correlation (−0.48; Table 2) is remarkable when compared with the other correlations in Table 1. Although the correlation between EOF2U and ACE or the TC frequency is insignificant, the TC track composites based on EOF2U (not shown) reveal a

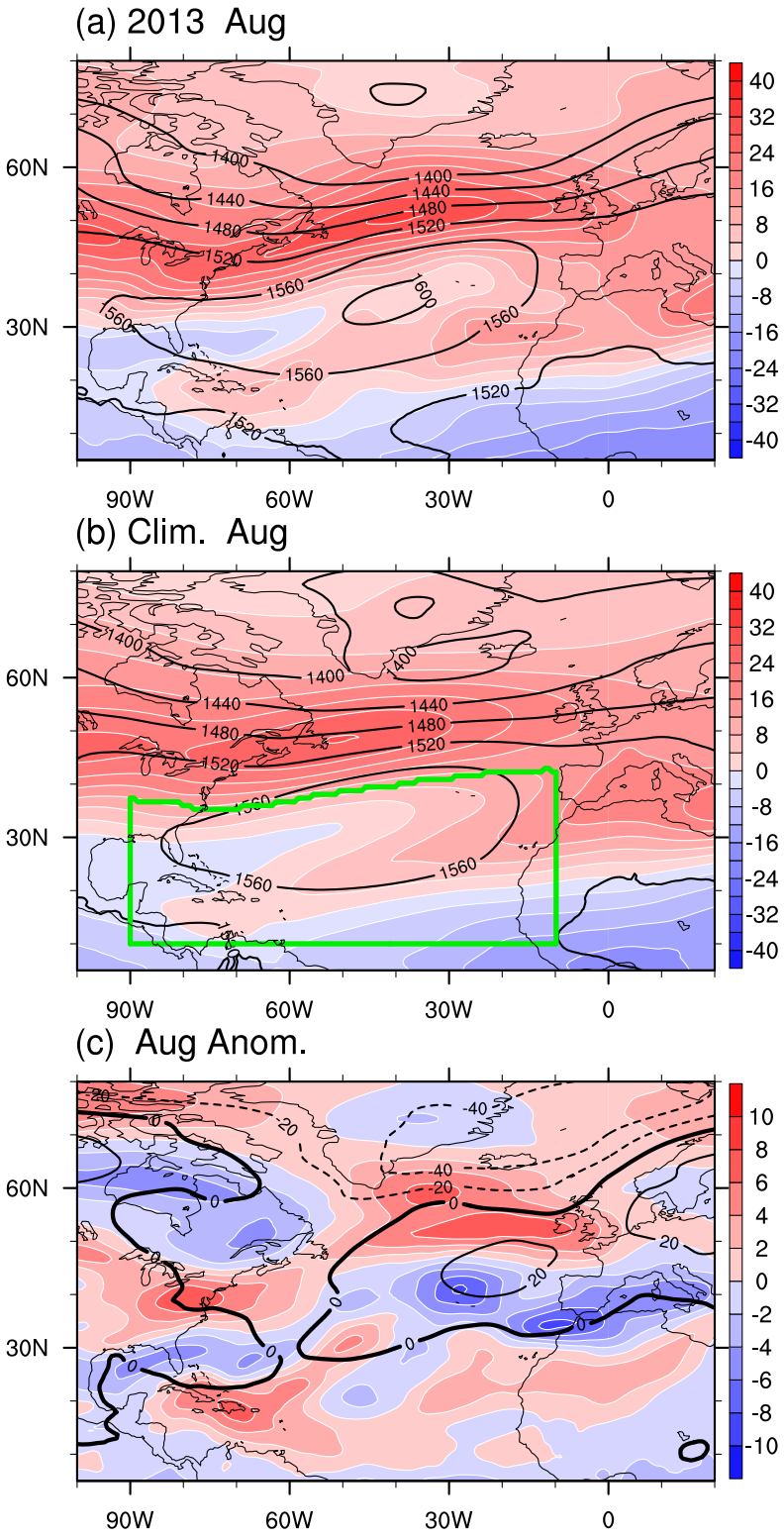

FIG. 8. The 200-hPa zonal wind (colored; m s^{-1}) and 850-hPa geopotential height (black contours; m) for (a) August 2013, (b) August climatology (1981–2010), and (c) their differences. The green line in (b) outlines the area where RWBFreq is defined.

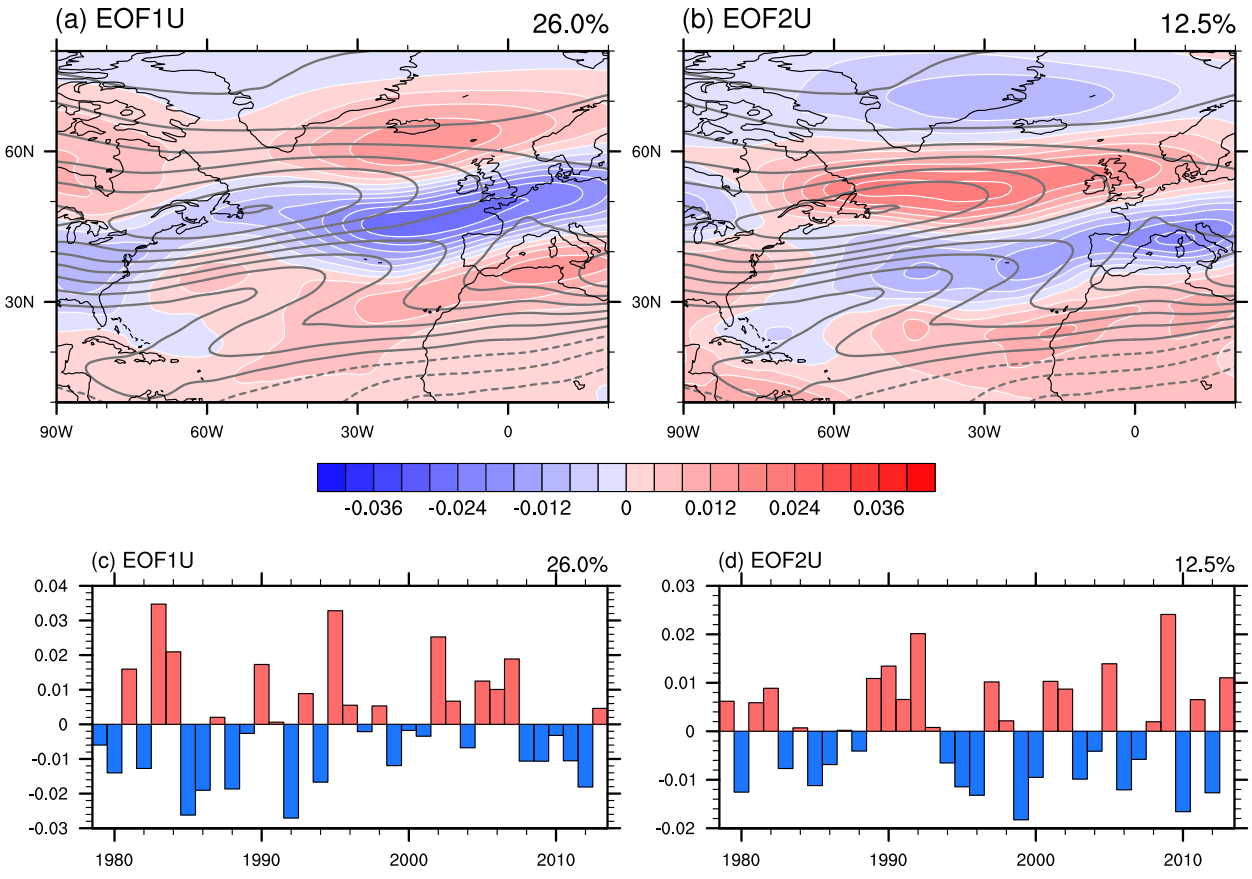

FIG. 9. (a),(b) Spatial patterns (shading) and (c),(d) time series of two leading modes of 200-hPa zonal wind; (left) EOF1U explains 26.0% of total variance and (right) EOF2U explains 12.5% of total variance. Gray contours in (a) and (b) represent the climatology of 200-hPa zonal wind.

strong contrast between the positive and negative phase of EOF2U. In the positive phase, when the midlatitude jet is stronger and RWB is active, 27 TCs formed, and 9 storms (33%) reached hurricane intensity. In contrast, 39 TCs developed in the negative phase of EOF2U, 23 of which (59%) strengthened into hurricanes.

EOF2U is weakly correlated to tropical Atlantic SST and only moderately correlated to Niño-3.4 (0.36), implying that EOF2U reflects the extratropical variability. Given the strong modulation of the midlatitude jet by the NAO in boreal winter, one may expect a strong linkage between EOF2U and the NAO. The relation between EOF2U and the NAO, however, is rather subtle. The NAO has strong seasonality (Portis et al. 2001), and the summertime NAO is not as well defined as the wintertime NAO (Folland et al. 2009). We examined two commonly used NAO indices, NAO/CPC (Barnston and Livezey 1987) and NAO/Jones (Jones et al. 1997). Unlike the wintertime, the two indices are only moderately correlated ($r \approx 0.41$) in August. Although both indices are significantly correlated with EOF2U, neither of the two NAO indices is significantly correlated with the Atlantic hurricane frequency (Table 1). The dipole pattern in the composites of the SLP based on the EOF2U (Fig. 10c) is similar to the second EOF mode of the summer seasonal mean SLP (Folland et al. 2009) or the so-called "mobile NAO" (Portis et al. 2001). However, our calculation showed that the second EOF mode of SLP in August (figure not shown) is not significantly correlated with the Atlantic hurricane frequency either. These analyses thus suggest that the impacts of EOF2U on Atlantic TCs cannot be

TABLE 2. Correlation coefficients of EOF1U and EOF2U with different indices in August 1979–2013. The index naming and coefficient formatting are as in Table 1.

	HurrN	TSN	ACE	MDR	Niño-3.4	NAO/CPC	NAO/Jones
EOF1U	−0.04	0.12	0.16	0.13	−0.02	**0.42**	−0.10
EOF2U	**−0.48**	−0.18	−0.28	−0.13	**0.36**	**0.35**	**0.63**

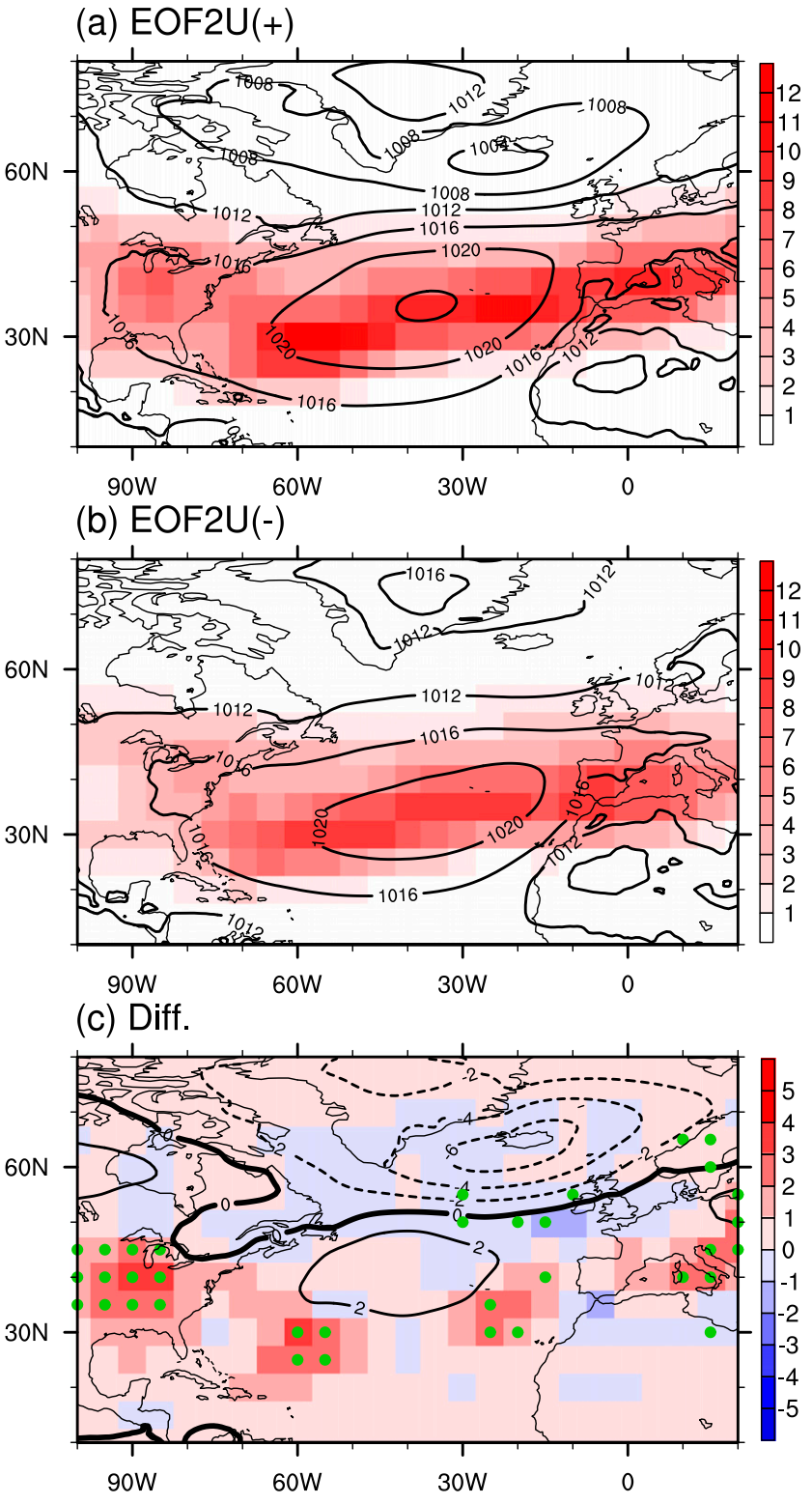

FIG. 10. Anticyclonic RWB frequency and sea level pressure for the (a) positive and (b) negative phases of EOF2U, and (c) their differences. Green dots highlight differences in RWB distribution that exceed the 90% confidence level.

TABLE A1. Predictions and observed activity of the 2013 Atlantic hurricane season.

Forecasting group	Forecasting method	Forecast issue date	Total named storms	Hurricanes	Accumulated cyclone energy (10^4 kt^2)
NOAA	Hybrid	23 May 2013	70% chance of 13–20	70% chance of 7–11	70% chance of 120%–205% of median
Florida State University (FSU) Center for Ocean–Atmosphere Prediction Studies (COAPS)	Dynamical	30 May 2013	15 (70% chance of 12–17)	8 (70% chance of 5–10)	135
Met Office	Dynamical	15 May 2013	14 (70% chance of 10–18)	9 (70% chance of 4–14)	130 (70% chance of 76–184)
Colorado State University	Statistical	3 Jun 2013	18	9	165
Tropical Storm Risk	Statistical	5 Apr 2013	15 (±4.1)	7.5 (±2.8)	131 (±55)
Weather Services International	Statistical	8 Apr 2013	16	9	—
2013 observed	—	—	13	2	33
Climatology, 1981–2011	—	—	12.3	6.5	104.4

simply attributed to the NAO or cannot be well represented by the commonly used NAO indices.

6. Summary and discussion

Despite the favorable tropical SST anomalies and active easterly waves over West Africa and the east Atlantic, TC activity over the Atlantic was substantially suppressed in August and early September of 2013, which led to a seasonal prediction bust. In this study, we focused on the month of August and investigated what disrupted the empirical relationship between tropical SST and Atlantic TCs. It was found that the dry and high-VWS conditions happened unusually frequently over the West MDR and hindered TC development. The mid- to upper-tropospheric dryness and high VWS can be attributed to the frequent equatorward intrusion of cold and dry extratropical air associated with anticyclonic RWB.

An index, RWBFreq, was defined based on the anticyclonic RWB frequency equatorward of the midlatitude jet axis over the North Atlantic. Composite analyses during 1979–2013 showed that dry air and strong vertical shear occur more frequently, and Atlantic TC activity is substantially suppressed in the positive phase of RWBFreq. Significant correlations were found between RWBFreq and various indices of TC activity, and the correlations are stronger than or comparable to the correlations between some commonly used climate factors and TC activity (Table 1).

The frequent occurrence of RWB in 2013 is related to a stronger westerly jet extending farther eastward over the extratropical Atlantic. To examine whether what happened in August 2013 is associated with a recurrent mode, we extracted the leading modes in the interannual variability of the 200-hPa zonal wind and examined their relations to RWB occurrence and TC activity. The second mode (EOF2U), which resembles the jet anomalies in 2013, modulates the basinwide RWB and is significantly correlated with the Atlantic hurricane frequency. In the positive phase of EOF2U, the Atlantic midlatitude jet sharpens and extends farther eastward; RWB tends to occur more frequently, and TC activity is suppressed significantly.

A limitation of this study is that we focused on the month of August. The EOF analyses for the other months (July, September, and October) did not reveal a pattern similar to EOF2U, likely because of the seasonality of the extratropical Atlantic circulation (e.g., Portis et al. 2001). However, our ongoing research indicates that the extratropics significantly impact Atlantic TCs via RWB throughout the hurricane season. The results will be reported in due course.

Despite the limitation, this study highlights the importance of extratropical impacts on the tropical and subtropical Atlantic, and it echoes the insightful statement by Galewsky et al. (2005): ''subtropical humidity could change independently of any tropical mechanism if changes in extratropical eddies change the statistics of the extratropical drying.'' We suspect that a similar statement can be made about the VWS as well. Our study also indicates that the extratropical impacts may be a missing piece in the seasonal prediction schemes of TC activity. The limited intrinsic predictability of extratropical variability may help to understand the uncertainties in tropical cyclone prediction. Or, more optimistically, the improved representation of extratropical processes may help to improve tropical cyclone seasonal predication. Further study is underway, investigating the variability and predictability of RWB frequency over the North Atlantic in the hurricane season, as well as their implications for the seasonal prediction of Atlantic TC activity.

Acknowledgments. This research is supported by the National Science Foundation Grant AGS-1118429, the Office of Naval Research Grant N00014-11-1-0446, and the Navy Research Laboratory Grant N00173-15-1-G004. The ERA-Interim data were made available by NCAR's Computational and Information Systems Laboratory Research Data Archive. We thank two anonymous reviewers for their constructive comments.

APPENDIX

Predicted and Observed TC Activity during the 2013 Atlantic Hurricane Season

Table A1 summarizes the predicted and the observed TC activity in the 2013 Atlantic hurricane season along with the long-term mean (from http://coaps.fsu.edu/hurricanes/forecast-archive). All models predicted an above-normal season in terms of the named TC count, hurricane count, and accumulated cyclone energy. Although the observed TC count is close to the long-term mean and not far from the predictions, the hurricane count is much lower than the predictions, and the observed ACE was only about 20% of the predicted values (Fogarty and Klotzbach 2014).

REFERENCES

Abatzoglou, J. T., and G. Magnusdottir, 2006: Planetary wave breaking and nonlinear reflection: Seasonal cycle and interannual variability. *J. Climate*, **19**, 6139–6152, doi:10.1175/JCLI3968.1.

Aiyyer, A. R., and C. Thorncroft, 2006: Climatology of vertical wind shear over the tropical Atlantic. *J. Climate*, **19**, 2969–2983, doi:10.1175/JCLI3685.1.

Barnston, A. G., and R. E. Livezey, 1987: Classification, seasonality and persistence of low-frequency atmospheric circulation patterns. *Mon. Wea. Rev.*, **115**, 1083–1126, doi:10.1175/1520-0493(1987)115<1083:CSAPOL>2.0.CO;2.

Bell, G. D., and Coauthors, 2000: Climate assessment for 1999. *Bull. Amer. Meteor. Soc.*, **81** (6), S1–S50, doi:10.1175/1520-0477(2000)81[s1:CAF]2.0.CO;2.

Blunden, J., and D. S. Arndt, 2014: State of the Climate in 2013. *Bull. Amer. Meteor. Soc.*, **95** (7), S1–S279, doi:10.1175/2014BAMSStateoftheClimate.1.

Braun, S. A., 2010: Reevaluating the role of the Saharan air layer in Atlantic tropical cyclogenesis and evolution. *Mon. Wea. Rev.*, **138**, 2007–2037, doi:10.1175/2009MWR3135.1.

Brown, R. G., and C. Zhang, 1997: Variability of midtropospheric moisture and its effect on cloud-top height distribution during TOGA COARE. *J. Atmos. Sci.*, **54**, 2760–2774, doi:10.1175/1520-0469(1997)054<2760:VOMMAI>2.0.CO;2.

Cangialosi, J., 2013: Tropical Storm Erin. National Hurricane Center Rep. AL052013, 11 pp.

Cau, P., J. Methven, and B. Hoskins, 2007: Origins of dry air in the tropics and subtropics. *J. Climate*, **20**, 2745–2759, doi:10.1175/JCLI4176.1.

Chen, J.-H., and S.-J. Lin, 2011: The remarkable predictability of inter-annual variability of Atlantic hurricanes during the past decade. *Geophys. Res. Lett.*, **38**, L11804, doi:10.1029/2011GL047629.

——, and ——, 2013: Seasonal predictions of tropical cyclones using a 25-km-resolution general circulation model. *J. Climate*, **26**, 380–398, doi:10.1175/JCLI-D-12-00061.1.

Dee, D. P., and Coauthors, 2011: The ERA-Interim reanalysis: Configuration and performance of the data assimilation system. *Quart. J. Roy. Meteor. Soc.*, **137**, 553–597, doi:10.1002/qj.828.

DeMaria, M., 1996: The effect of vertical shear on tropical cyclone intensity change. *J. Atmos. Sci.*, **53**, 2076–2088, doi:10.1175/1520-0469(1996)053<2076:TEOVSO>2.0.CO;2.

Doblas-Reyes, F. J., and M. Déqué, 1998: A flexible bandpass filter design procedure applied to midlatitude intraseasonal variability. *Mon. Wea. Rev.*, **126**, 3326–3335, doi:10.1175/1520-0493(1998)126<3326:AFBFDP>2.0.CO;2.

Dritschel, D. G., and M. E. McIntyre, 2008: Multiple jets as PV staircases: The Phillips effect and the resilience of eddy-transport barriers. *J. Atmos. Sci.*, **65**, 855–874, doi:10.1175/2007JAS2227.1.

Dunion, J. P., 2011: Rewriting the climatology of the tropical North Atlantic and Caribbean Sea atmosphere. *J. Climate*, **24**, 893–908, doi:10.1175/2010JCLI3496.1.

Dunkerton, T. J., and R. K. Scott, 2008: A barotropic model of the angular momentum–conserving potential vorticity staircase in spherical geometry. *J. Atmos. Sci.*, **65**, 1105–1136, doi:10.1175/2007JAS2223.1.

——, M. T. Montgomery, and Z. Wang, 2009: Tropical cyclogenesis in a tropical wave critical layer: Easterly waves. *Atmos. Chem. Phys.*, **9**, 5587–5646, doi:10.5194/acp-9-5587-2009.

Elsner, J. B., 2003: Tracking hurricanes. *Bull. Amer. Meteor. Soc.*, **84**, 353–356, doi:10.1175/BAMS-84-3-353.

Fitzpatrick, P. J., J. A. Knaff, C. W. Landsea, and S. V. Finley, 1995: Documentation of a systematic bias in the aviation model's forecast of the Atlantic tropical upper-tropospheric trough: Implications for tropical cyclone forecasting. *Wea. Forecasting*, **10**, 433–446, doi:10.1175/1520-0434(1995)010<0433:DOASBI>2.0.CO;2.

Fogarty, C. T., and P. Klotzbach, 2014: The 2013 Atlantic hurricane season: Blip or flip? [in "State of the Climate in 2013"]. *Bull. Amer. Meteor. Soc.*, **95** (7), ES106–ES107.

Folland, C. K., J. Knight, H. W. Linderholm, D. Fereday, S. Ineson, and J. W. Hurrell, 2009: The summer North Atlantic Oscillation: Past, present, and future. *J. Climate*, **22**, 1082–1103, doi:10.1175/2008JCLI2459.1.

Fritz, C., and Z. Wang, 2013: A numerical study of the impacts of dry air on tropical cyclone formation: A development case and a nondevelopment case. *J. Atmos. Sci.*, **70**, 91–111, doi:10.1175/JAS-D-12-018.1.

Galarneau, T. J., R. McTaggart-Cowan, L. F. Bosart, and C. A. Davis, 2015: Development of North Atlantic tropical disturbances near upper-level potential vorticity streamers. *J. Atmos. Sci.*, **72**, 572–597, doi:10.1175/JAS-D-14-0106.1.

Galewsky, J., A. Sobel, and I. Held, 2005: Diagnosis of subtropical humidity dynamics using tracers of last saturation. *J. Atmos. Sci.*, **62**, 3353–3367, doi:10.1175/JAS3533.1.

Ge, X., T. Li, and M. Peng, 2013: Effects of vertical shears and midlevel dry air on tropical cyclone developments. *J. Atmos. Sci.*, **70**, 3859–3875, doi:10.1175/JAS-D-13-066.1.

Goldenberg, S. B., and L. J. Shapiro, 1996: Physical mechanisms for the association of El Niño and West African rainfall with Atlantic major hurricane activity. *J. Climate*, **9**, 1169–1187, doi:10.1175/1520-0442(1996)009<1169:PMFTAO>2.0.CO;2.

——, C. W. Landsea, A. M. Mestas-Nuñez, and W. M. Gray, 2001: The recent increase in Atlantic hurricane activity: Causes and implications. *Science*, **293**, 474–479, doi:10.1126/science.1060040.

Gray, W. M., 1984a: Atlantic seasonal hurricane frequency. Part I: El Niño and 30 mb Quasi-Biennial Oscillation influences. *Mon. Wea. Rev.*, **112**, 1649–1668, doi:10.1175/1520-0493(1984)112<1649:ASHFPI>2.0.CO;2.

——, 1984b: Atlantic seasonal hurricane frequency. Part II: Forecasting its variability. *Mon. Wea. Rev.*, **112**, 1669–1683, doi:10.1175/1520-0493(1984)112<1669:ASHFPI>2.0.CO;2.

——, 1990: Strong association between West African rainfall and U.S. landfall of intense hurricanes. *Science*, **249**, 1251–1256, doi:10.1126/science.249.4974.1251.

Hankes, I., Z. Wang, G. Zhang, and C. Fritz, 2014: Merger of African easterly waves and formation of Cape Verde storms. *Quart. J. Roy. Meteor. Soc.*, **141**, 1306–1319, doi:10.1002/qj.2439.

Hartmann, D. L., and P. Zuercher, 1998: Response of baroclinic life cycles to barotropic shear. *J. Atmos. Sci.*, **55**, 297–313, doi:10.1175/1520-0469(1998)055<0297:ROBLCT>2.0.CO;2.

Holton, J. R., 2004: *An Introduction to Dynamic Meteorology*. 4th ed. International Geophysics Series, Vol. 88, Academic Press, 535 pp.

Hopsch, S. B., C. D. Thorncroft, K. Hodges, and A. Aiyyer, 2007: West African storm tracks and their relationship to Atlantic tropical cyclones. *J. Climate*, **20**, 2468–2483, doi:10.1175/JCLI4139.1.

——, ——, and K. R. Tyle, 2010: Analysis of African easterly wave structures and their role in influencing tropical cyclogenesis. *Mon. Wea. Rev.*, **138**, 1399–1419, doi:10.1175/2009MWR2760.1.

Janowiak, J. E., 1988: An investigation of interannual rainfall variability in Africa. *J. Climate*, **1**, 240–255, doi:10.1175/1520-0442(1988)001<0240:AIOIRV>2.0.CO;2.

Jensen, M. P., and A. D. Del Genio, 2006: Factors limiting convective cloud-top height at the ARM Nauru Island Climate Research Facility. *J. Climate*, **19**, 2105–2117, doi:10.1175/JCLI3722.1.

Jones, P. D., T. Jonsson, and D. Wheeler, 1997: Extension of the North Atlantic oscillation using early instrumental pressure observations from Gibraltar and south-west Iceland. *Int. J. Climatol.*, **17**, 1433–1450, doi:10.1002/(SICI)1097-0088(19971115)17:13<1433::AID-JOC203>3.0.CO;2-P.

Kalnay, E., and Coauthors, 1996: The NCEP/NCAR 40-Year Reanalysis Project. *Bull. Amer. Meteor. Soc.*, **77**, 437–471, doi:10.1175/1520-0477(1996)077<0437:TNYRP>2.0.CO;2.

Kim, H.-M., and P. J. Webster, 2010: Extended-range seasonal hurricane forecasts for the North Atlantic with a hybrid dynamical-statistical model. *Geophys. Res. Lett.*, **37**, L21705, doi:10.1029/2010GL044792.

Klotzbach, P. J., and W. M. Gray, 2009: Twenty-five years of Atlantic basin seasonal hurricane forecasts. *Geophys. Res. Lett.*, **36**, L09711, doi:10.1029/2009GL037580.

Kossin, J. P., and D. J. Vimont, 2007: A more general framework for understanding Atlantic hurricane variability and trends. *Bull. Amer. Meteor. Soc.*, **88**, 1767–1781, doi:10.1175/BAMS-88-11-1767.

——, S. J. Camargo, and M. Sitkowski, 2010: Climate modulation of North Atlantic hurricane tracks. *J. Climate*, **23**, 3057–3076, doi:10.1175/2010JCLI3497.1.

Landsea, C. W., and J. L. Franklin, 2013: Atlantic hurricane database uncertainty and presentation of a new database format. *Mon. Wea. Rev.*, **141**, 3576–3592, doi:10.1175/MWR-D-12-00254.1.

LaRow, T., L. Stefanova, D.-W. Shin, and S. Cocke, 2010: Seasonal Atlantic tropical cyclone hindcasting/forecasting using two sea surface temperature datasets. *Geophys. Res. Lett.*, **37**, L02804, doi:10.1029/2009GL041459.

Latif, M., N. Keenlyside, and J. Bader, 2007: Tropical sea surface temperature, vertical wind shear, and hurricane development. *Geophys. Res. Lett.*, **34**, L01710, doi:10.1029/2006GL027969.

Lee, S.-K., D. B. Enfield, and C. Wang, 2011: Future impact of differential interbasin ocean warming on Atlantic hurricanes. *J. Climate*, **24**, 1264–1275, doi:10.1175/2010JCLI3883.1.

McIntyre, M. E., and T. N. Palmer, 1983: Breaking planetary waves in the stratosphere. *Nature*, **305**, 593–600, doi:10.1038/305593a0.

Nakamura, H., 1994: Rotational evolution of potential vorticity associated with a strong blocking flow configuration over Europe. *Geophys. Res. Lett.*, **21**, 2003–2006, doi:10.1029/94GL01614.

Portis, D. H., J. E. Walsh, M. E. Hamly, and P. J. Lamb, 2001: Seasonality of the North Atlantic oscillation. *J. Climate*, **14**, 2069–2078, doi:10.1175/1520-0442(2001)014<2069:SOTNAO>2.0.CO;2.

Postel, G. A., and M. H. Hitchman, 1999: A climatology of Rossby wave breaking along the subtropical tropopause. *J. Atmos. Sci.*, **56**, 359–373, doi:10.1175/1520-0469(1999)056<0359:ACORWB>2.0.CO;2.

Rayner, N. A., D. E. Parker, E. B. Horton, C. K. Folland, L. V. Alexander, D. P. Powell, E. C. Kent, and A. Kaplan, 2003: Global analyses of sea surface temperature, sea ice, and night marine air temperature since the late nineteenth century. *J. Geophys. Res.*, **108**, 4407, doi:10.1029/2002JD002670.

Roca, R., R. Guzman, J. Lemond, J. Meijers, L. Picon, and H. Brogniez, 2012: Tropical and extra-tropical influences on the distribution of free tropospheric humidity over the intertropical belt. *Surv. Geophys.*, **33**, 565–583, doi:10.1007/s10712-011-9169-4.

Scott, R. K., D. G. Dritschel, L. M. Polvani, and D. W. Waugh, 2004: Enhancement of Rossby wave breaking by steep potential vorticity gradients in the winter stratosphere. *J. Atmos. Sci.*, **61**, 904–918, doi:10.1175/1520-0469(2004)061<0904:EORWBB>2.0.CO;2.

Strong, C., and G. Magnusdottir, 2008: Tropospheric Rossby wave breaking and the NAO/NAM. *J. Atmos. Sci.*, **65**, 2861–2876, doi:10.1175/2008JAS2632.1.

Swanson, K. L., 2008: Nonlocality of Atlantic tropical cyclone intensities. *Geochem. Geophys. Geosyst.*, **9**, Q04V01, doi:10.1029/2007GC001844.

Takemi, T., O. Hirayama, and C. Liu, 2004: Factors responsible for the vertical development of tropical oceanic cumulus convection. *Geophys. Res. Lett.*, **31**, L11109, doi:10.1029/2004GL020225.

Tang, B., and K. Emanuel, 2012: Sensitivity of tropical cyclone intensity to ventilation in an axisymmetric model. *J. Atmos. Sci.*, **69**, 2394–2413, doi:10.1175/JAS-D-11-0232.1.

Thorncroft, C. D., B. J. Hoskins, and M. E. McIntyre, 1993: Two paradigms of baroclinic-wave life-cycle behaviour. *Quart. J. Roy. Meteor. Soc.*, **119**, 17–55, doi:10.1002/qj.49711950903.

Tyner, B., and A. Aiyyer, 2012: Evolution of African easterly waves in potential vorticity fields. *Mon. Wea. Rev.*, **140**, 3634–3652, doi:10.1175/MWR-D-11-00170.1.

Vecchi, G. A., and B. J. Soden, 2007: Effect of remote sea surface temperature change on tropical cyclone potential intensity. *Nature*, **450**, 1066–1070, doi:10.1038/nature06423.

——, and Coauthors, 2014: On the seasonal forecasting of regional tropical cyclone activity. *J. Climate*, **27**, 7994–8016, doi:10.1175/JCLI-D-14-00158.1.

Vitart, F., and Coauthors, 2007: Dynamically-based seasonal forecast of Atlantic tropical storm activity issued in June by EUROSIP. *Geophys. Res. Lett.*, **34**, L16815, doi:10.1029/2007GL030740.

Wang, H., J. K. E. Schemm, A. Kumar, W. Wang, L. Long, M. Chelliah, G. D. Bell, and P. Peng, 2009: A statistical forecast model for Atlantic seasonal hurricane activity based on the NCEP dynamical seasonal forecast. *J. Climate*, **22**, 4481–4500, doi:10.1175/2009JCLI2753.1.

Wang, Z., M. T. Montgomery, and T. J. Dunkerton, 2009: A dynamically-based method for forecasting tropical cyclogenesis location in the Atlantic sector using global model products. *Geophys. Res. Lett.*, **36**, L03801, doi:10.1029/2008GL035586.

——, ——, and C. Fritz, 2012: A first look at the structure of the wave pouch during the 2009 PREDICT–GRIP dry runs over the Atlantic. *Mon. Wea. Rev.*, **140**, 1144–1163, doi:10.1175/MWR-D-10-05063.1.

——, G. Zhang, M. S. Peng, J. Chen, and S. Lin, 2015: Predictability of Atlantic tropical cyclones in the GFDL HiRAM model. *Geophys. Res. Lett.*, **42**, 2547–2554, doi:10.1002/2015GL063587.

Waugh, D. W., 2005: Impact of potential vorticity intrusions on subtropical upper tropospheric humidity. *J. Geophys. Res.*, **110**, D11305, doi:10.1029/2004JD005664.

Yang, H., and R. T. Pierrehumbert, 1994: Production of dry air by isentropic mixing. *J. Atmos. Sci.*, **51**, 3437–3454, doi:10.1175/1520-0469(1994)051<3437:PODABI>2.0.CO;2.

Zhang, C., B. E. Mapes, and B. J. Soden, 2003: Bimodality in tropical water vapour. *Quart. J. Roy. Meteor. Soc.*, **129**, 2847–2866, doi:10.1256/qj.02.166.

Zhang, G., and Z. Wang, 2013: Interannual variability of the Atlantic Hadley circulation in boreal summer and its impacts on tropical cyclone activity. *J. Climate*, **26**, 8529–8544, doi:10.1175/JCLI-D-12-00802.1.

Zhao, M., I. M. Held, and G. A. Vecchi, 2010: Retrospective forecasts of the hurricane season using a global atmospheric model assuming persistence of SST anomalies. *Mon. Wea. Rev.*, **138**, 3858–3868, doi:10.1175/2010MWR3366.1.